

## Neutron production by 200 mJ ultrashort laser pulses

G. Pretzler,<sup>1</sup> A. Saemann,<sup>1</sup> A. Pukhov,<sup>1</sup> D. Rudolph,<sup>2</sup> T. Schätz,<sup>2</sup> U. Schramm,<sup>2</sup> P. Thirolf,<sup>2</sup> D. Habs,<sup>2</sup> K. Eidmann,<sup>1</sup>  
G. D. Tsakiris,<sup>1</sup> J. Meyer-ter-Vehn,<sup>1</sup> and K. J. Witte<sup>1</sup>

<sup>1</sup>Max-Planck-Institut für Quantenoptik, D-85748 Garching, Germany

<sup>2</sup>Sektion Physik, LMU München, Am Coulombwall 1, D-85748 Garching, Germany

(Received 27 October 1997; revised manuscript received 30 January 1998)

We report the observation of neutrons released from  $d(d,n)^3\text{He}$  fusion reactions in the focus of 200 mJ, 160 fs Ti:sapphire laser pulses on a deuterated polyethylene target. Optimizing the fast electron and ion generation by applying a well-defined prepulse led to an average rate of 140 neutrons per shot. Furthermore, the production of a substantial number of MeV  $\gamma$  rays could be observed. The occurrence of neutrons and  $\gamma$  rays is attributed to the formation and explosion of a relativistic plasma channel in the laser focus, which is confirmed by numerical calculations. [S1063-651X(98)08507-9]

PACS number(s): 52.50.Jm, 52.60.+h, 52.25.Tx, 29.25.Dz

The production of neutrons in laser plasmas by fusion of fast deuterium ions was first reported in the 1970s (e.g., [1]), when high-power lasers of ns-pulse duration were used. Later, high yields of neutrons were generated by thermonuclear fusion in the compressed core of inertial confinement fusion pellets driven by huge laser installations of energies exceeding 10 kJ [2]. Very recently, it has been shown that by employing ps pulses the energy needed to produce large numbers of neutrons can be significantly reduced [3]. However, this type of experiment is still restricted to single-shot operation because of the large size of the involved lasers.

In the last decade, the rapid development of ultrashort-pulse chirped-pulse amplification (CPA) lasers has suddenly opened up a broad field of high-intensity table-top experiments. Nowadays, laser systems delivering pulses at a high repetition rate with energies in the 100-mJ range and duration of about 100 fs are routinely used in many laboratories throughout the world. A key point is that when these pulses are focused into an underdense plasma channel formation is possible which may lead to an enhancement of the focus intensity.

First, CPA-laser pulses have sufficient power to readily exceed the threshold for relativistic self-focusing [4]  $P_{th} \approx 17 \times 10^9 \text{ W} (\omega/\omega_p)^2$ , where  $\omega$  is the laser frequency and  $\omega_p$  is the plasma frequency. Relativistic self-focusing leads to an increase of the refractive index due to the relativistic mass increase of electrons quivering in the focal region. The medium then acts as a positive lens, producing an increase of focal intensity and, depending on the laser pulse and plasma parameters, either filamentation or self-channeling of the pulse occurs [5].

Second, if the dimensionless amplitude  $a = eA/mc^2$  of the vector potential  $A$  ( $e$  and  $m$  are the charge and rest mass of the electron, and  $c$  is the velocity of light) enters the relativistic regime  $a \geq 1$  (which corresponds roughly to a focal intensity of  $10^{18} \text{ W/cm}^2$ , also achieved by table-top CPA lasers), electrons are accelerated in forward rather than transverse direction, as postulated in [6]. These electrons favor effectively the self-enhancement of the focus intensity as shown recently by three-dimensional particle-in-cell (3D PIC) simulations [7]. A considerable part of the electrons are accelerated to multi-MeV energies in the laser direction and

generate multimegagauss magnetic fields leading to self-pinching of both the electrons and the light field. The key result is that a *single narrow light propagation channel* is created with a diameter of a few wavelengths which is elongated over many Rayleigh lengths.

Recent experiments confirmed these predictions: The acceleration of electrons to the multi-MeV level in the forward direction was proved in several experiments [8]. Single-channel formation in an underdense plasma was evidenced in [9], and a clear correlation between electron acceleration and channel formation was demonstrated in [10].

The fair agreement between these experiments and theory suggests that the process of relativistic channel formation is conceptually understood. Therefore, we may go one step further and use this effect for triggering high-energy experiments like nuclear reactions. For example, the generated MeV electrons may be converted into high fluxes of MeV  $\gamma$  radiation [11] or used for the production of positrons or fission neutrons based on cascaded processes as proposed in [12]. A more straightforward method is to directly use the hot plasma channel itself for high-energy experiments. In this paper, neutrons were produced in a deuterium plasma by the fusion reaction  $\text{D} + \text{D} \rightarrow {}^3\text{He} (0.82 \text{ MeV}) + n(2.45 \text{ MeV})$ . The occurrence of neutrons in the experiment implies the acceleration of deuterium ions to a few hundreds of keV. Our simulations suggest that this enormous acceleration is achieved when the channel explodes radially behind the light pulse. Hence this channel itself is proved to be an interesting tool for doing a new class of table-top experiments combining lasers and nuclear physics.

The experiments were carried out at the Max-Planck-Institut für Quantenoptik using the ATLAS Ti:sapphire laser system delivering 160-fs, 200-mJ pulses at a central wavelength of 790 nm in 10-Hz operation. These pulses were focused into a focal spot of  $4.5 \mu\text{m}$  diameter (full width at half maximum of the intensity) by a gold-coated  $f/3$  off-axis parabolic mirror, yielding a peak intensity of the order of  $10^{18} \text{ W/cm}^2$ . For neutron production the use of a well defined prepulse (see Fig. 1) proved to be crucial. This prepulse contained 15% of the beam energy arriving at the target 300 ps before the main pulse. The prepulse focus diameter was  $20 \mu\text{m}$ , leading to a prepulse intensity of roughly

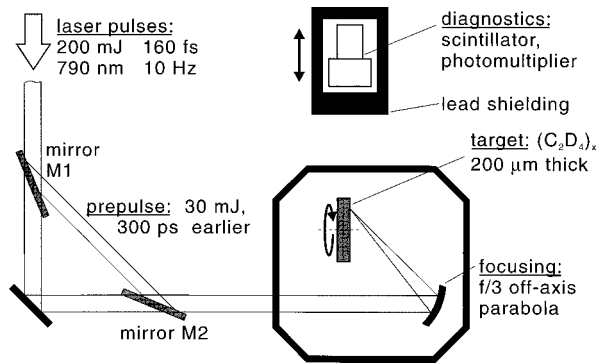


FIG. 1. Experimental setup for the production and detection of D-D fusion neutrons. A well-defined prepulse was established by partially inserting the mirrors  $M1$  and  $M2$  into the beam from below. The distance of the diagnostics (including shielding) from the target was varied, and the diagnostics axis was roughly in the plane of the target (at  $45^\circ$  to the incident laser).

$10^{16}$  W/cm $^2$ . The laser angle of incidence onto the target was set to  $45^\circ$ , leading to a strong  $p$ -polarized component which is expected to have a high level of absorption for the prepulse on the target surface leading to efficient preplasma formation. The main pulse focus was carefully adjusted into the center of the prepulse focus thus providing a *homogeneous preplasma* for the main pulse.

The target material was deuterated polyethylene powder [ $(C_2D_4)_x$ , D enrichment  $>98\%$ ] pressed into a flat layer of about  $200\text{-}\mu\text{m}$  thickness on a rough Al substrate at  $90^\circ\text{C}$  under 50 bars pressure. The target was mounted on a rotating holder for irradiating a fresh surface with each laser shot.

A NE213 liquid scintillator (area  $0.02\text{ m}^2$ , depth  $0.1\text{ m}$ ) coupled to a fast photomultiplier was used for neutron detection (efficiency 30% for neutrons and close to 100% for  $\gamma$  rays). The signal was read out by a 1-GHz oscilloscope (Tektronix TDS 684B). For preventing the  $\gamma$  signal from saturating the multiplier, the detector was shielded by 20 cm lead towards the target and 10 cm on the other sides.

The readout system was triggered by the laser pulse and measurements were performed at four different distances. The main results are presented in Fig. 2 and reveal three features: A first strong peak is only slightly dependent on the detector distance, a second peak is significantly delayed with increasing distance, and a broad noiselike structure appears at even later times.

Each of the curves in Fig. 2 was obtained by measuring the time delay of the leading edge of all the detected pulses on several raw data records. For most shots the data contained only the first peak. For evaluation only those data files were selected which contained signals in addition to the first peak.

The first peak is identified as a  $\gamma$  signal due the short delay time (corresponding to the light velocity) and by the fact that this peak was strongly influenced by the lead shielding. With a shielding of 20 cm lead we got an order of 1  $\gamma$ -photon per shot at a distance of 2 m, corresponding to a total number of a few  $10^7$   $\gamma$  quanta in the MeV range per shot into the full solid angle (assuming isotropic emission, a maximum transmission through the 20 cm lead shield of  $\approx 10^{-4}$  at  $h\nu \approx 2\text{--}3$  MeV and a detector efficiency close to 1). Reduction of the lead shield thickness enhanced the  $\gamma$

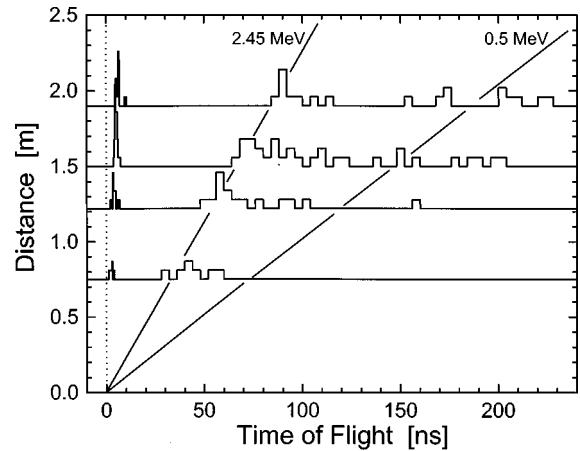


FIG. 2. Temporal distribution of the number of detected pulses at several distances of the detector from the target (sampling interval  $0.4\text{ ns}$  for the  $\gamma$  peak,  $4\text{ ns}$  everywhere else). Only those single data files were selected for evaluation in which signals other than the  $\gamma$  peak (first peak) were detected. The expected delays for neutrons with two different energies are indicated by the two straight lines. The second peak in each readout represents  $2.45\text{ MeV}$  D-D fusion neutrons. Note that no other significant monoenergetic neutron signal is apparent.

peak considerably causing saturation of the photomultiplier.

The second peak was not significantly influenced by the lead. Fitting the time delay to the distance yields a velocity of  $2.2 \times 10^7$  m/s, which is in good agreement with  $2.45\text{ MeV}$  neutrons produced by the D-D fusion reaction at threshold. The probability of detecting a neutron peak was quadratically decreasing with detector distance. At a distance of 1 m it took an average of 15 shots to see a neutron signal. With a solid angle fraction of  $1/625$  at this distance, a detection efficiency of 30%, and assuming isotropic neutron distribution we obtained an average of 140 neutrons per shot. The quadratic decrease with distance is strong evidence that the laser focus is indeed the source of the neutrons (as opposed to mechanisms that accelerate ions out of the target for reactions at other locations, e.g., the target chamber wall).

Besides the peak corresponding to the  $2.45\text{ MeV}$  neutrons we also observed single peaks at larger delays. They are attributed to slower neutrons without a preferential velocity. An explanation of these late events as photoneutrons (deuterium disintegration either by  $\gamma$  rays or by electrons) is ruled out by the low cross sections of these processes [13] and by the fact that the majority of such photoneutrons would have very low energies and would appear much later in time. A Monte Carlo simulation of the propagation of the fusion neutrons under our experimental conditions using the code as described in [14] yielded a temporal spectrum similar to that observed. The origin of the temporal smearing is a delay and energy loss caused by scattering of the neutrons at the target chamber walls and the concrete laboratory floor.

We note that the shot-to-shot fluctuations were strong, such that pileup of the neutron signal occurred more often than expected from the average rates. Therefore, the given average neutron yield constitutes a *lower limit*. A similar effect was observed for the  $\gamma$  signal. The strong fluctuations may be attributed to target inhomogeneities or to laser energy fluctuations, which were in the range of  $\pm 15\%$  and

may hence strongly influence the self-focusing behavior of the main laser pulse (see below).

Best results were achieved with the main pulse focus placed about  $50\ \mu\text{m}$  in front of the target, i.e., in the optimal self-focusing region as calculated by the simulations presented below. Without a prepulse, no neutrons were detected and the probability for detecting  $\gamma$  rays decreased by at least one order of magnitude. We note that the roughness of the target surface turned out not to be a crucial parameter since when irradiating a used surface of the target a comparable neutron yield was obtained. This finding can be understood in that only the preplasma formation is influenced by the surface conditions, while the conditions for the creation of the relativistic plasma channel remain rather unchanged.

The proper choice of the various experimental parameters was supported by intensive numerical simulations. The development of the preplasma was calculated by the modified hydrocode MULTI-FS [15], yielding an expansion velocity of  $10^7\ \text{cm/s}$  and hence a plasma scale length of  $30\ \mu\text{m}$  after 300 ps, when the main pulse arrives. The interaction of the main pulse with this preplasma was calculated using the 3D-electromagnetic relativistic PIC code Virtual Laser Plasma Laboratory [7] (VLPL 3D) employing 64 processors of the CRAY T3E at Rechenzentrum Garching, Germany. These calculations used the actual experimental values concerning laser pulse shape, focus intensity, and preplasma density. One result of the simulation is that the actual focus intensity of about  $10^{18}\ \text{W/cm}^2$  proved to be sufficient to produce a relativistic channel. This self-focusing of the laser main pulse in the underdense preplasma (approximately at a density of  $n_e = 10^{21}\ \text{cm}^{-3}$  which is half the critical density) leads to a factor-of-5 increase in intensity as compared to the intensity resulting from the focusing mirror only. The electromagnetic fields in this region create a significant number of relativistic electrons in the MeV range [see Fig. 3(a)] which escape predominantly into the forward direction.

These electrons when stopped in the thick Al substrate behind the  $(\text{C}_2\text{D}_4)_x$  foil generate MeV bremsstrahlung  $\gamma$  rays. The number of  $\gamma$  quanta created may be roughly estimated from

$$N_\gamma = N_e \sigma_\gamma \rho d / M_{\text{Al}}. \quad (1)$$

With  $N_e \approx 10^{10}$  (number of fast electrons),  $\sigma_\gamma \approx 10^{-25}\ \text{cm}^2$  (cross section for the generation of MeV quanta),  $\rho d \approx 2\ \text{g/cm}^2$  (stopping range for MeV electrons in solid Al [16]), and  $M_{\text{Al}} = 4.5 \times 10^{-23}\ \text{g}$  (atomic mass of aluminum), we find  $N_\gamma \approx 5 \times 10^7$ , which is in reasonable agreement with the measurement. These estimations were confirmed by a more detailed calculation using the Monte Carlo code GEANT [17]. Figure 3(a) shows the resulting spectrum of generated  $\gamma$  rays. Furthermore, the calculations yield the angular dependence of the  $\gamma$  radiation, showing that the high-energy parts of the spectrum are focused in the forward direction, while the sub-MeV energy range is mainly reabsorbed in the surrounding material.

According to the PIC simulations, the major part of the absorbed energy is contained in the electrons within and around the high-intensity light channel. The high electron temperature [see Fig. 3(a)] generates strong space charge fields which accelerate the deuterium ions from the plasma

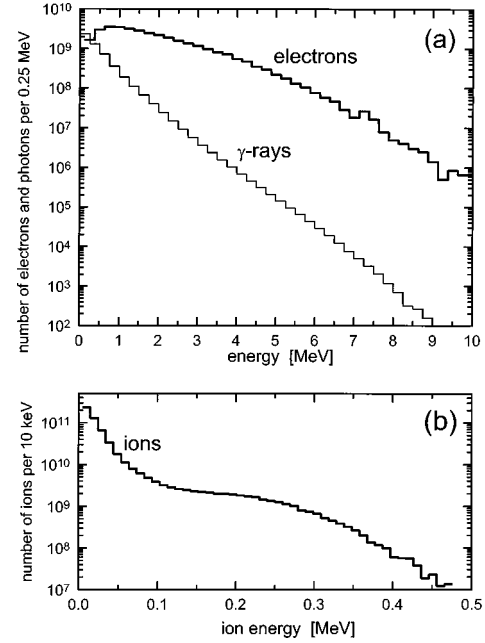


FIG. 3. (a) Spectrum of electrons produced in the focus of a  $2 \times 10^{18}\ \text{W/cm}^2$ , 160 fs laser pulse in a preformed plasma as calculated by the VLPL 3D PIC code, and bremsstrahlung  $\gamma$  rays generated in 5-cm-thick Al behind the laser focus as calculated by the GEANT code. (b) Deuterium ion spectrum 750 fs after the laser pulse calculated by the PIC code.

channel radially outwards in a kind of a radial explosion. The ion energy distribution is shown in Fig. 3(b). The accelerated deuterium ions collide with cold deuterium ions in the surrounding preplasma leading to the release of neutrons via the fusion reaction  $d(d,n)\ ^3\text{He}$ . To estimate the number of neutrons we assume the surrounding preplasma to be homogeneous within a radius of  $r_p \approx 20\ \mu\text{m}$  corresponding to the prepulse spot size and to have a density of cold deuterium ions of  $n_{d,\text{cold}} \approx 10^{20}\ \text{cm}^{-3}$ . We note that energy losses of the fast deuterium ions by elastic collisions when they propagate through the preplasma are negligible because their mean free path (estimated from Ref. [18]) largely exceeds the preplasma radius. With these assumptions the number of neutrons is given by

$$N_n = N_{d,\text{fast}} \langle \sigma_f \rangle r_p n_{d,\text{cold}}, \quad (2)$$

where  $N_{d,\text{fast}} = 4 \times 10^{10}$  is the number of fast ions [Fig. 3(b)] and  $\langle \sigma_f \rangle = 28\ \text{mb}$  is the cross section of the D-D fusion reaction [19] weighted with the energy distribution of the deuterium ions. With these numbers we find a total rate of 220 neutrons per shot.

We note that the size and the gradient of the preplasma and the intensity in the laser focus are important input parameters for the simulations. Due to the uncertainty involved in the actual values of these parameters, the simulations are expected to describe the experimental results within better than an order of magnitude. Therefore, and in view of the rough assumptions made for the final estimation, the agreement of calculated and measured values can be considered to be satisfactory.

In conclusion, we demonstrated that a 160-fs laser pulse with an energy of only 200 mJ is able to trigger nuclear fusion reactions and to produce neutrons. This is achieved by channeling and self-focusing in a carefully shaped preplasma. The experiment is table-top and was done with a 10-Hz repetition rate. We note that our focus parameters are close to the threshold for the onset of the hot channel formation. Therefore, a moderate increase in focus intensity promises a large increase in neutron yield. As to the number of  $\gamma$  quanta and fusion neutrons, good agreement was achieved between theory and experiment. The experimental results

can hence supply valuable information on the effects resulting from relativistic hot channel formation.

This research was supported in part by the Commission of the European Communities within the framework of the Association Euratom–Max-Planck-Institut für Plasmaphysik. Thanks are due to M. Groß for Monte-Carlo simulations, to the University of Cologne for providing the neutron detector, and to H. Haas, A. Böswald, and P. Sachsenmeier for technical support. The help of W. Fuß with target production is gratefully acknowledged.

- 
- [1] F. Floux *et al.*, Phys. Rev. A **1**, 821 (1970); K. Büchl *et al.*, in *Proceedings of the 4th International Conference on Plasma Physics and Controlled Nuclear Fusion Research*, edited by R. Schenin and J. W. Weil (IAEA Vienna, 1971), Vol. 1, p. 645.
- [2] J. Lindl, Phys. Plasmas **2**, 3933 (1995).
- [3] P. A. Norreys *et al.*, Plasma Phys. Controlled Fusion **40**, 175 (1998).
- [4] C. E. Max *et al.*, Phys. Rev. Lett. **33**, 209 (1974); H. Hara *et al.*, J. Opt. Soc. Am. **65**, 882 (1975); G. Z. Sun, Phys. Fluids **30**, 526 (1987); A. B. Borisov *et al.*, Phys. Rev. Lett. **68**, 2309 (1992).
- [5] P. Monot *et al.*, Phys. Rev. Lett. **74**, 2953 (1995); A. B. Borisov *et al.*, Plasma Phys. Controlled Fusion **37**, 569 (1995).
- [6] E. S. Sarachik and G. T. Schappert, Phys. Rev. D **1**, 2738 (1970); P. B. Corkum *et al.*, in *Atoms in Intense Laser Fields*, edited by M. Gavrila (Academic Press, New York, 1992), p. 109.
- [7] A. Pukhov and J. Meyer-ter-Vehn, Phys. Rev. Lett. **76**, 3975 (1996).
- [8] D. Umstadter *et al.*, Science **273**, 472 (1996); A. Modena *et al.*, Nature (London) **377**, 606 (1995); G. Malka *et al.*, Phys. Rev. Lett. **79**, 2053 (1997).
- [9] M. Borghesi *et al.*, Phys. Rev. Lett. **78**, 879 (1996).
- [10] R. Wagner *et al.*, Phys. Rev. Lett. **78**, 3125 (1997).
- [11] J. D. Kmetec *et al.*, Phys. Rev. Lett. **68**, 1527 (1992).
- [12] P. L. Shkolnikov *et al.*, Appl. Phys. Lett. **71**, 3471 (1997).
- [13] R. Moreh *et al.*, Phys. Rev. C **39**, 1247 (1993); D. Harder *et al.*, Phys. Lett. **32B**, 610 (1970).
- [14] A general Monte Carlo  $N$ -particle transport code, MCNF, edited by J. F. Briesmeister, Los Alamos National Laboratory Report No. LA-12625-M (unpublished).
- [15] R. Ramis *et al.*, Comput. Phys. Commun. **49**, 475 (1988).
- [16] L. V. Spencer, Natl. Bur. Stan. (U.S.) Monograph No. 1 (U.S. GPO, Washington, D.C., 1959), Vol. 1.
- [17] *GEANT User's Guide*, edited by R. Brun *et al.*, CERN Report No. DD/EE/82 (unpublished).
- [18] K. Nishikawa and M. Wakatani, *Plasma Physics*, 2nd ed. (Springer Verlag, Berlin, 1993).
- [19] S. Glasstone and R. H. Lovberg, *Controlled Thermonuclear Reactions* (D. van Nostrand, Princeton, NJ, 1960).